STRUCTURE AND PROPERTIES OF ION-PLASMA DEPOSITED FILMS OF CoCrFeMiMn HIGH-ENTROPY ALLOY

O.I. Kushnerov*, S.I. Ryabtsev, V.F. Bashev

Oles Honchar Dnipro National University, Dnipro, Ukraine
**e-mail: kushnrv@gmail.com*

High-entropy $Co_{19}Cr_{18}Fe_{22}Mn_{21}Ni_{20}$ thin films were obtained by the modernized method of three-electrode ion-plasma sputtering of mosaic targets consisting of pure metals. The structure, electrical resistance, and magnetic properties of films were investigated. Single diffuse halo was seen on the XRD patterns of the as-deposited films, which confirms their amorphous structure. Some of the thin films, which were annealed at 900 K in a vacuum, were identified to be oxidized by a small amount of oxygen in the work chamber. After the heat treatment, the $Co_{19}Cr_{18}Fe_{22}Mn_{21}Ni_{20}$ films were transformed from an amorphous state into a crystallized FCC solid solution with the lattice parameter a=0.3613 nm. Also, the cubic B2 phase of FeCo with a lattice parameter of 0.2857 nm was formed in the annealed films. As a result of oxidation processes, a dispersed phase of manganese oxide also arose after annealing. The temperature dependencies of electrical resistivity of films were measured by the four-point technique upon continuously heating in the high vacuum. Both as-deposited and annealed films clearly revealed a typical ferromagnetic behavior. The as-deposited high-entropy film exhibited the soft magnetic properties while the annealed films could be attributed to hard magnetic materials.

Keywords: high-entropy alloy, amorphous and nanocrystalline structure, thin film, magnetic properties, electrical resistance, electron microscopy, X-ray diffraction.

Received 02.11.2022; Received in revised form 08.12.2022; Accepted 23.12.2022

1. Introduction

In 2004 the first papers on the study of high-entropy alloys (HEAs) were published (today along with term "HEA" definitions of multi-principal element alloys (MPEAs) and complex concentrated alloys (CCAs) are also used [1-3]). The HEAs are composed of at least 5 major components with equiatomic or nearly equiatomic concentrations which are between 5 and 35 at. % [1-3]. Due to the high mixing entropy, multicomponent HEAs typically consist of simple solid solutions with BCC or FCC lattices. At the same time, the selection of components makes it possible to obtain the structure of HEA, which is a combination of a simple solid solution, characterized by a high plasticity, and intermetallic compounds, characterized by high hardness. The HEAs are characterized by unique structures and many useful service characteristics, such as hardness, wear resistance, resistance to oxidation, corrosion, and ionizing radiation, high thermal stability, and biocompatibility [1-6]. Thus, HEAs are promising as materials for use in electronics, atomic energy, transport equipment, rocket and space technology, medicine, etc. The majority of HEAs were investigated in the as-quenched or homogenized state, while much less attention was paid to the study of thin films of high-entropy alloys (HEFs). However, recently such research has received much more attention. HEFs not only have excellent performance as HEAs, but even some of the properties have been enhanced [7]. HEFs have shown great potentials for application in the fields of high hardness coating, corrosion-resistant coating, diffusion barriers in the integrated circuit systems, etc. In the present work, the metastable states and properties of $Co_{19}Cr_{18}Fe_{22}Mn_{21}Ni_{20}$ high-entropy thin films are discussed.

2. Experimental details

The HEFs with a nominal composition $Co_{19}Cr_{18}Fe_{22}Mn_{21}Ni_{20}$ (in at. %) have been synthesized by the modernized method of three-electrode ion-plasma sputtering of composite targets. The cooling rate, which relates to the relaxation time of individual atoms on the substrate, was in this case theoretically evaluated to be 10^{12}-10^{14} K/s. Sputtering was carried out on the sitall substrates, as well as on a fresh cleavage of NaCl single crystals.

The sputtering deposition process was carried out at room temperature with a pure Ar

atmosphere, the working pressure was controlled at $5 \cdot 10^{-2}$ Pa. The deposition rate for the HEA thin film was 0.19 nm/s. The as-deposited HEA film thickness was estimated to be ~ 110 nm. Films deposited on single-crystal substrates after the dissolution of the salt were used for structural studies by X-ray diffraction analysis (with a photographic registration, in a Debye camera on the URS-2.0 diffractometer in filtered Co K_α radiation). Debyegrams were digitally microphotometered and processed using a qualitative phase analysis software Qualx2. Films obtained under identical conditions of deposition on the sitall substrates were used to study the thermal stability and physical properties of nonequilibrium structures. The temperature dependencies of electrical resistivity of films were measured by the four-point technique upon continuously heating in the high vacuum with a pressure of $4 \cdot 10^{-2}$ Pa. The magnetic properties of the HEFs were measured by a vibrating sample magnetometer (VSM) at room temperature with the magnetic field applied parallel to the film plane.

3. Results and discussion

The XRD patterns of the films are shown in Fig. 1. Single diffuse halo observed on the XRD patterns of the as-deposited films confirms their amorphous structure. The coherently scattering domain size (crystallite size) of films estimated by the Sherer equation ($L= K\lambda/\beta\cos\theta$) is ~ 4 nm. Some of the thin films annealed at 900 K in a vacuum furnace were identified to be oxidized by a small amount of oxygen in the chamber (as pointed in [8], all the as-deposited thin films contained 7–8 at % oxygen which was from the deposition process). These films transform from an amorphous state into a crystallized FCC solid solution structure with the lattice parameter a=0.3613 nm with coherently scattering domain size ~30 nm, on the base of FCC-iron. Such crystalline structure was reported earlier for the bulk as-casted samples and thin films (with the lattice parameter of 0.359 nm for the as-casted sample) of $Co_{20}Cr_{20}Fe_{20}Mn_{20}Ni_{20}$ alloy [9,10]. The cubic B2 phase of FeCo with a lattice parameter of 0.2857 nm is also formed in the annealed films. The occurrence of this phase was noted in the study of CoCuFeNiMn samples subjected to prolonged annealing at 500°C [10]. As a result of oxidation processes, a dispersed phase of cubic FCC manganese oxide MnO is also formed after annealing because of diffusion of atoms and oxidation.

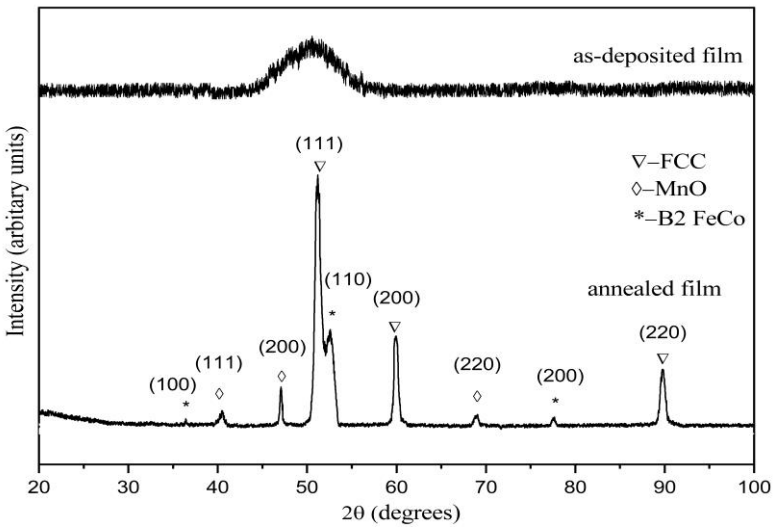

Fig.1. XRD patterns of $Co_{19}Cr_{18}Fe_{22}Mn_{21}Ni_{20}$ HEA films

Let us consider the temperature dependence of the relative electrical resistivity of the films. The temperatures of the single - stage phase transformations (crystallization

processes) in $Co_{19}Cr_{18}Fe_{22}Mn_{21}Ni_{20}$ films are ~ 540 K for heating rate 4.5 K/min and ~ 580 K for heating rate 9 K/min. The mean activation energy of phase transitions (E_A), calculated by the Kissinger method is ~ 6100 K (50.7 kJ/mol). This value is several times lower than determined for the decay of nonequilibrium structures in alloys obtained by quenching from the liquid state. It should be mentioned that this feature is characteristic of films obtained by quenching from the vapor phase. Obviously, it is due to the increased contribution of surface diffusive processes. The films in the initial amorphous state are characterized by a very low value of the temperature coefficient of resistance (average value ~$3.5 \cdot 10^{-5}$ 1/K, while after crystallization it increases up to $5.1 \cdot 10^{-4}$ 1/K.

In Fig. 2 the magnetic hysteresis loops of the as-deposited and annealed $Co_{19}Cr_{18}Fe_{22}Mn_{21}Ni_{20}$ high-entropy films measured at room temperature are presented. Both resemble typical ferromagnetic behavior. The as-deposited HEA film shows the soft magnetic properties and the saturation magnetization (*Ms*), and coercivity (*Hc*) are 29.4 $A \cdot m^2/kg$ and 400 A/m. After annealing the values of these parameters increase, respectively, to 57.6 $A \cdot m^2/kg$ and 8760 A/m. So, the annealed films can be referred to hard magnetic materials.

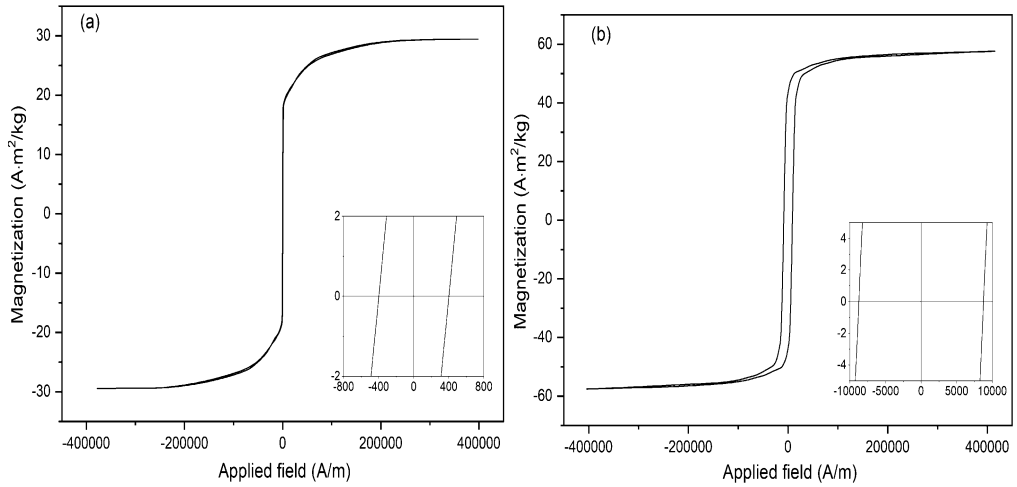

Fig. 2. Hysteresis loops of $Co_{19}Cr_{18}Fe_{22}Mn_{21}Ni_{20}$ HEA films: (a) as-deposited; (b) annealed.

Compared with the magnetic properties of CoCuFeNiMn HEA in some of the available literature [11], the $Co_{19}Cr_{18}Fe_{22}Mn_{21}Ni_{20}$ HEA films show much higher saturation magnetizations. On the other hand, the CoCuFeNiMn samples obtained by mechanical alloying showed an even greater value of the magnetization 94.29 $A \cdot m^2/kg$ [12]. A relatively high value of magnetization obtained in $Co_{19}Cr_{18}Fe_{22}Mn_{21}Ni_{20}$ films and its growth after annealing can be explained considering that the saturation magnetization *M* of the alloy depends mainly on structure and composition, specifically, the magnetic exchange interaction. For example, Mn and Cr addition dramatically reduce the magnetization *M* of CoFeNi because they favor the antiferromagnetic order with the other elements in this alloy. Thus, the crystallization is accompanied by structure coarsening, and phase transformation could result in magnetic property changes. The key role in the increase of magnetization is obviously played by the FeCo phase, which is characterized by high values of saturation magnetization. Forming the minor phase of manganese oxide also should contribute to the fact that the antiferromagnetic order associated with Mn atoms is suppressed to favor ferromagnetism. The increase of *Hc* is also taking place evidently due to the formation of the microcrystalline structure contained a lot of defects and nanoprecipitates, which hampers the domain walls displacements during magnetization reversal.

4. Conclusions

High-entropy films with a nominal composition $Co_{19}Cr_{18}Fe_{22}Mn_{21}Ni_{20}$ have been deposited successfully by the modernized method of three-electrode ion-plasma sputtering of composite targets. XRD patterns of the as-deposited films confirm their amorphous structure. Some of the thin films, which were annealed at 900 K in a vacuum furnace, were found to be oxidized by a small amount of oxygen in the chamber. These films transform into a crystallized FCC solid solution structure with the lattice parameter a = 0.3613 nm. A minor phase of manganese oxide is also formed after annealing together with the B2 phase of FeCo. Investigations of the temperature dependence of electrical resistivity have shown that the films in the initial amorphous state are characterized by a very low value of the temperature coefficient of resistance ($3.5 \cdot 10^{-5}$ 1/K). The magnetic properties of as-deposited and annealed $Co_{19}Cr_{18}Fe_{22}Mn_{21}Ni_{20}$ films have been investigated by a vibrating sample magnetometer. The as-deposited HEA films are the soft magnetics, the annealed films can be referred to semi-hard magnetic materials.

References

1. High entropy alloys. Innovations, advances, and applications / T.S. Srivatsan, M. Gupta. – Boca Raton : CRC Press, 2020.–758 p.

2. High-entropy materials: theory, experiments, and applications / J. Brechtl, P.K. Liaw. – Cham : Springer International Publishing, 2021. — 774 p.

3. **Miracle, D.B.** A critical review of high entropy alloys and related concepts / D.B. Miracle, O.N. Senkov // Acta Materialia. – 2017. – Vol. 122. – P. 448 – 511.

4. **Kushnerov, O.I.** Structure and physical properties of cast and splat-quenched CoCr0.8Cu0.64FeNi high entropy alloy / O.I. Kushnerov, V.F. Bashev // East European Journal of Physics. – 2021. – No. 3. –P. 43 – 48.

5. **Kushnerov, O.I.** Structure and properties of nanostructured metallic glass of the Fe–B–Co–Nb–Ni–Si high-entropy alloy system / O. I. Kushnerov, V. F. Bashev, S. I. Ryabtsev // Springer Proceedings in Physics. – 2021. – P. 557 – 567.

6. **Polonskyy, V.A.** Structure and corrosion-electrochemical properties of Fe-based cast high-entropy alloys / V.A. Polonskyy, V.F. Bashev, O.I. Kushnerov // Journal of Chemistry and Technologies. – 2020. – Vol. 28, No. 2. – P. 177 – 185.

7. **Yan, X. H.** A brief review of high-entropy films / X. H. Yan, J. S. Li, W. R. Zhang, Y. Zhang // Materials Chemistry and Physics. – 2018. – Vol. 210. – P. 12 – 19.

8. **Yang, Y.-C.** Influence of Ti content on the partial oxidation of TixFeCoNi thin films in vacuum annealing / Y.-C. Yang, J.-W. Yeh, C.-H. Tsau // Materials. – 2017. – Vol. 10, No. 10. – P. 1141.

9. **Mridha, S.** Nanomechanical behavior of CoCrFeMnNi high-entropy alloy / S. Mridha, S. Das, S. Aouadi, S. Mukherjee, R. S. Mishra // JOM. –2015. – Vol. 67, No. 10. – P. 2296 – 2302.

10. **Otto, F.** Decomposition of the single-phase high-entropy alloy CrMnFeCoNi after prolonged anneals at intermediate temperatures / F. Otto, A. Dlouhý, K.G. Pradeep, M. Kuběnová, D. Raabe, G. Eggeler, E. P. George // Acta Materialia. – 2016. – Vol. 112. – P. 40 – 52.

11. **Zuo, T.** Tailoring magnetic behavior of CoFeMnNix (x = Al, Cr, Ga, and Sn) high entropy alloys by metal doping / T. Zuo, M. C. Gao, L. Ouyang, X. Yang, Y. Cheng, R. Feng, S. Chen, P. K. Liaw, J. A. Hawk, Y. Zhang // Acta Materialia. – 2017. – Vol. 130. – P. 10 – 18.

12. **Ji, W.** Alloying behavior and novel properties of CoCrFeNiMn high-entropy alloy fabricated by mechanical alloying and spark plasma sintering / W. Ji, W. Wang, H. Wang, J. Zhang, Y. Wang, F. Zhang, Z. Fu // Intermetallics. – 2015. –Vol. 56. – P. 24 – 27.